Study on Performance of Detonation-Driven Shock Tube*

Akio YAMANAKA**, Yosuke ARIGA**,
Tetsuro OBARA***, Pin CAI***
and Shigeharu OHYAGI***

A detonation-driven shock tube firstly designed by H.R. Yu is considered to be a useful apparatus for producing high-enthalpy flow. In this apparatus, a strong shock wave is generated by detonating an oxygen-hydrogen mixture (oxy-hydrogen) and the driver gas temperature and pressure are extremely high compared with those of a conventional shock tube. However, the structure of the detonation wave is not uniform, e.g., the detonation wave has three-dimensional cellular structures and multiple transverse waves. Furthermore, the detonation wave is followed by a Taylor expansion fan and the performance of detonation-driven shock tube is not well understood. In this preliminary study, a detonation-driven shock tube is constructed and its performance is experimentally investigated by measuring pressure histories and the profile of the ionization current behind the detonation wave. As a result, (i) the pressure history of the detonation wave is clarified and shows reasonable agreement with the result obtained by the KASIMIR shock tube simulation code. (ii) The propagation velocity of the detonation wave coincides well with the theoretical prediction assuming a Chapman-Jouguet detonation wave. (iii) The equivalence ratio of the oxy-hydrogen mixture to produce the highest Mach number of the shock wave is evaluated to be $\phi \simeq 1.7$.

Key Words: Combustion, Detonation, Shock Wave, Shock Tube, Detonation Driver, Mach Number

1. Introduction

The supersonic combustion RAM (SCRAM) jet engine has attracted attention because of its potential for use in next-generation for space plane, and hypersonic airliners. This engine is operated by mixing fuel and air in a supersonic flow field, and is required to undergo stable combustion[1]-[3]. In order to investigate the combustion flow field inside this engine, it is necessary to generate a high-enthalpy flow field in the laboratory[2],[3].

A shock tunnel is a facility for generating such a high-enthalpy flow field with comparable ease, even though the duration of the high-enthalpy flow is short[4]. This facility utilizes high-pressure and high-temperature gases behind a reflected shock wave that is produced by rupturing the diaphragm between a high-pressure reservoir and a low-pressure channel. In order to generate such a high-enthalpy flow, it is required to produce a shock wave of high-propagation Mach number. In a simple shock tube, a shock wave with high-propagation Mach number is generated by increasing the pressure ratio p_4/p_1 of high-pressure reservoir p_4 to low-pressure tube p_1. The propagation Mach number $M_{S,\max}$ of the shock wave is calculated by a simple shock tube theory represented by the following equation, assuming that pressure ratio is infinity, namely, $p_4/p_1 \to \infty$[5],

$$M_{S,\max}=\frac{1}{2}\frac{\kappa_1+1}{\kappa_4-1}\frac{a_4}{a_1}+\sqrt{\left\{\frac{1}{2}\left(\frac{\kappa_1+1}{\kappa_4-1}\right)\frac{a_4}{a_1}\right\}^2+1}\,, \tag{1}$$

where subscript 1 indicates low-pressure chamber

* Received 11th December, 2001. Japanese original: Trans. Jpn. Soc. Mech. Eng., Vol. 66, No. 651, B (2000), pp. 2992-2998 (Received 22nd October, 1999)

** Graduate Student, Graduate School of Science and Engineering, Saitama University, 255 Shimo-Ohkubo, Saitama-shi, Saitama 338-8570, Japan

*** Department of Mechanical Engineering, Faculty of Engineering, Saitama University, 255 Shimo-Ohkubo, Saitama-shi, Saitama 338-8570, Japan. E-mail: tobara@mech.saitama-u.ac.jp

(driven gas), subscript 4 a high-pressure chamber (driver gas), κ the ratio of specific heat, and a the speed of sound. Therefore, the Mach number of a shock wave is approximated as,

$$M_{S,\max} \simeq \frac{\kappa_1+1}{\kappa_4-1}\sqrt{\frac{\kappa_4}{\kappa_1}\frac{w_1}{w_4}\frac{T_4}{T_1}}, \qquad (2)$$

where w is molecular weight of the gas and T absolute temperature[5]. Therefore, a strong shock wave of high-propagation Mach number is produced by choosing high-temperature light gas as high-pressure reservoir gas and the pressure ratio p_4/p_1 is increased to as high a value as possible. However, it is unacceptable to assume $p_4/p_1 \to \infty$ from the restriction of the strength of the material used for the shock tube apparatus; thus an upper limit for the propagation Mach number of the shock wave must exist. For instance, the propagation Mach number of the shock wave is calculated as $M_S \simeq 3$ by setting the pressure ratio at $p_4/p_1 \simeq 100$, and by letting the driver gas be helium and driven gas, air.

On the other hand, a shock wave of high-propagation Mach number is produced easily by detonating an oxy-hydrogen mixture, since the gas behind a detonation wave is the driver gas, and is a state of high pressure and high temperature. The temperature ratio T_4/T_1 as shown in Eq.(2) can be increased by using the detonation reaction. For example, the temperature behind the Chapman-Jouguet (C-J) detonation wave is calculated to be 3 700 K for a stoichiometric oxy-hydrogen mixture (equivalence ratio, $\phi=1.0$) and initial pressure $p_{4i}=101$ kPa. The temperature ratio is approximately 3.5 times higher than that of the simple shock tube in which the temperature ratio is unity.

This detonation-driven shock tube was designed for the first time by Yu[6],[7], and it has the advantage that a shock wave of high-propagation Mach number can be generated with a relatively small pressure ratio between the high-pressure reservoir and the low-pressure tube. It has been reported that the oxy-hydrogen ignition method is critical[7], and the numerical simulation technique is useful for the prediction of the Mach number of the induced shock wave[8]. A numerical simulation was carried out to investigate the performance of converging detonation drivers[9]. Furthermore, it was demonstrated that the Taylored condition can be obtained by adjusting the pressure ratio between driver to driven gas and the composition of driver gas[8]. However, because the detonation wave has three-dimensional cellular structures[10], the detonation driver has disadvantages such that uniformity behind the detonation wave is not sufficient compared with that in the simple shock tube. Furthermore, the rupture timing of a diaphragm installed between the detonation driver and the shock tube is very important because the detonation wave is followed by a Taylor expansion wave, and temperature and pressure behind detonation wave decrease with time. Therefore, the performance of the detonation-driven shock tube is investigated in detail herein.

In this research, a detonation-driven shock tube was designed and experiments were carried out to clarify the performance of the detonation-driven shock tube. Firstly, the Mach number of the shock wave was considered to be strongly influenced by the rupturing condition of the diaphragm installed between the driver section and the shock tube. Then, the material and the depth of the cross-ditch carved on the diaphragm were varied. Pressure histories behind the detonation wave and the shock wave were compared with the results obtained by the KASIMIR shock tube simulation program[11].

2. Experimental

2.1 Apparatus

Figure 1 shows a schematic diagram of the experimental setup. A detonation-driven shock tube is constructed from an initiation tube (inner diameter $ID=30$ mm, length $L=1\,000$ mm), a driver tube ($ID=50$ mm, $L=4\,500$ mm), a dump tube ($ID=50$ mm, $L=2\,100$ mm), a shock tube ($ID=50$ mm, $L=4\,200$ mm) made of stainless steel (SUS304), an observation section and a dump tank ($V=0.75\,\mathrm{m}^3$). The total length of this detonation-driven shock tube is approximately 14 m. A Schelkin spiral coil is inserted at the top part of the initiation tube to promote transition from deflagration to the detonation wave in a short distance. A detonation wave is generated inside the initiation tube when oxy-hydrogen gas mixture is ignited by a igniter. The detonation wave propagates in the driver tube, and the diaphragm is ruptured by high-temperature and high-pressure gas behind the detonation wave. Then, a shock wave is driven to the shock tube. The detonation wave propagating to the left is attenuated inside the dump tube that was evacuated beforehand.

Four measuring stations are installed on the initiation tube (named IP1~IP4), eight stations are installed on the driver tube (DP1~DP8), and four sta-

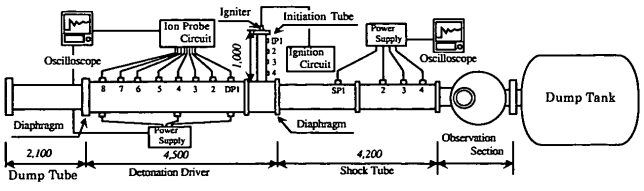

Fig. 1 Schematic diagram of the detonation-driven shock tube

tions are installed on the shock tube (SP1~SP4). Three piezoelectric pressure transducers (PCB Co., Ltd., 113A24, rise time: 1 μs) are mounted on the driven tube and four pressure transducers are mounted on the shock tube in order to measure the propagation velocity of the detonation and the shock wave. Ionization probes are mounted on the initiation tube and the detonation tube diametrically opposed to the pressure transducers for the detection of the arrival time of the detonation wave. The area between the two iron cores of 1.4 mm diameter (gap: 1.0 mm, length: 2.5 mm) of the ionization probes is charged with 90 V DC voltage, and the two iron cores become electrically conductive behind the detonation wave because the gas behind the detonation wave is locally ionized[12),(13)]. The output signal from pressure transducers and ionization probes is stored using two oscilloscopes (Yokogawa Electric Co., DL1540, 200 MS/s), and is processed by a personal computer.

2.2 Method and conditions

The experimental conditions are shown in Table 1. The driver gas was oxy-hydrogen mixture and the equivalence ratio ϕ was varied from 1.0 to 2.0. The initial pressure of the driver gas p_{4i} was varied from 101 to 303 kPa. The driven gas was air, and the initial pressure was fixed at p_1=11.3 kPa. The diaphragm between the driver tube and the dump tube, and that between the driver tube and the shock tube were respectively partitioned using Mylar film of 75 μm thickness and a copper disk plate of 0.4 mm thickness. On the surface of the copper plate, a cross-ditch was carefully shaped beforehand in order to shorten the rupture time and to increase the opening area. It was necessary to equalize the depth and shape of the cross-ditch for obtaining high reproducibility in the experiment. Therefore, an air grinder (Nitto Kohki Co., Ltd., Airsonic L-35R, edge angle of blade: 90°, 30 000 rpm) was used for precisely shaping the cross-ditch on the copper plate by sliding it using an optical stage (Sigma Koki, Co., Ltd., Rack and Pinion Dovetail Stages). After shaping the cross-ditch, the depth of each cross-ditch was measured using a cross-sectional shape-measuring device (Kosaka Co., Surfcorder SE-3C, measurement error: 1 μm). The results showed that the standard deviation of the depth was 29% or less and this indicated that the cross-ditch had sufficiently high reproducibility. In the experiment, the depth of the cross-ditch δ was varied to be either 0.1 mm or 0.2 mm.

Table 1 Experimental conditions

	Driver Gas	Driven Gas
Species	H_2, O_2	Air
Equivalence Ratio, ϕ	1.0 ~ 2.0	-
Pressure (kPa)	$101 < p_{4i} < 303$	$p_1 = 11.3$

2.3 Preparation of driver gas

From the results of preliminary experiments, it was clarified that high reproducibility was obtained by improving the mixing conditions of oxy-hydrogen. Then, a premixing tank was fabricated, which was equipped with rotating wings driven by magnetic force. The premixing tank (200 mm inner diameter, length: 715 mm, volume: 2.25×10^{-2} m^3) was made of stainless steel (SUS304) and equipped with two rotating wings made of aluminum plates (600×70 mm). On the rotating wings were embedded 15 pieces of magnets, (Nd-Fe-B, surface magnetic flux density: 4 000 G, diameter: 5 mm, length: 10 mm) and the wings were then rotated at 23 rpm in order to promote the mixing of oxy-hydrogen.

Figure 2 illustrates the results of the equivalence ratio for direct filling in the driver tube, as measured by gas chromatography (Shimadzu Co., GC-8AIT). The vertical axis shows the equivalence ratio ϕ of driver gas, and the horizontal axis, the distance D from a igniter. By measuring the partial pressures of oxygen and hydrogen utilizing a strain pressure gauge (Nagano Keiki Co., Ltd., Digital pressure gauge GC-61), the gases are filled in order to obtain equivalent ratio ϕ=1.0 and pressure p_{4i}=101.3 kPa. This figure shows the case of utilizing the premixing tank (○), and the direct filling into the driver tube (▽). The equivalent ratio shows a large scatter over the distance investigated in the case of direct filling. In contrast, the equivalent ratio is almost uniform when the oxy-hydrogen mixture is filled through the premixing tank with stirring for 5 min. Therefore, it is confirmed that the equivalence ratio is $\phi=1.0\pm0.06$, and the driver gas is filled using this procedure throughout this study.

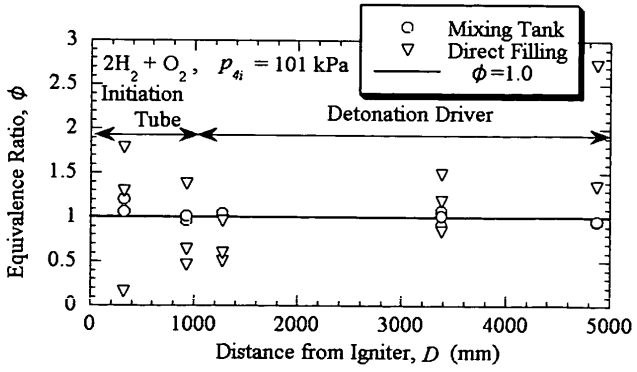

Fig. 2 Distribution of equivalence ratio ϕ with distance from igniter, D (p_{4i}=101 kPa)

3. Results and Discussion

3.1 Wave diagram

Figure 3 is a wave diagram of the detonation-driven shock tube, calculated by the KASIMIR shock tube simulation program[11]. The horizontal axis x shows the position of the detonation-driven shock tube, and the vertical axis is the time from the start of calculation. The initial conditions for the calculation are the same as the experimental conditions, assuming that the gas in the driver tube is oxy-hydrogen mixture with equivalence ratio $\phi=1.0$ and initial pressure $p_{4i}=101$ kPa. The dump tube is evacuated, and the gas inside the shock tube is air with initial pressure $p_1=11.3$ kPa. Furthermore, this calculation assumes that the diaphragm between the driver and shock tubes ruptures at ignition. A detonation wave (DW) propagates leftward from position $x=0$ instantaneously. A Taylor expansion wave (TE) follows the detonation wave. The detonation wave is reflected as an expansion wave (EW) and propagates rightward, since acoustic impedance is markedly changed between the driver tube and the dump tube. In the meantime, the detonation wave transforms to a shock wave in the dump tube and propagates leftward, and the reflected shock wave (RS) is generated at the left end of the dump tube. The shock wave (SW) propagates almost simultaneously rightward in the shock tube with the onset of calculation. The propagation velocity of the shock wave is not constant and decreases from the beginning of the propagation. This is because the expansion wave generated by the rupture of the diaphragm follows the shock wave, and pressure and temperature behind the shock wave are decreased. This phenomenon is qualitatively similar to the phenomenon that the contact surface (CS) follows the shock wave. The propagation velocity of the detonation wave is approximately 2 853 m/s and this is equal to the C-J detonation velocity. The propagation velocity of the shock wave is calculated to be 1 589 m/s, and this corresponds to Mach number $M_S=4.6$.

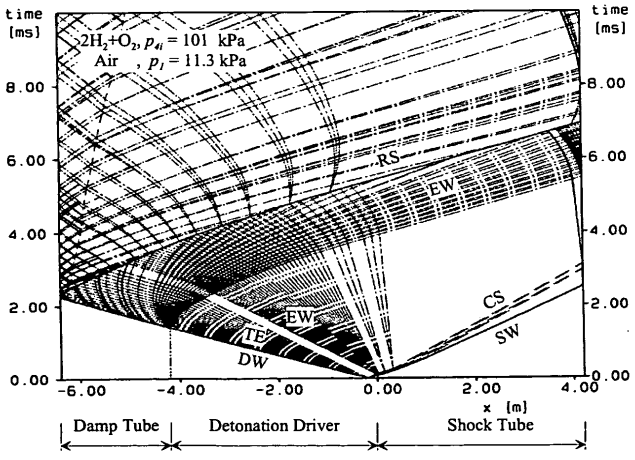

Fig. 3 Wave diagram of detonation-driven shock tube calculated by KASIMIR shock tube simulation code ($p_{4i}=101$ kPa, $p_1=11.3$ kPa, $\phi=1.0$)

3.2 Pressure histories in detonation driver

Figure 4 shows output signals from ionization probes mounted at IP1~IP4, DP1~DP8 (upper trace), and pressure histories (lower three traces) measured at stations DP1, DP4 and DP8 under experimental conditions $p_{4i}=303$ kPa and $\phi=1.0$. The output signal from the ionization probe is periodic confirming that a detonation wave of constant velocity is produced within a short distance from the igniter (detonation-induced distance $D_{id}<200$ mm). Furthermore, it is possible to confirm that the detonation wave is generated, based on the result that the output signals from the ionization probes agree with the rise time of the pressure histories. The maximum pressure behind the detonation wave is increased as it propagates from DP1 through DP8. This is because quenching of the detonation wave partially occurs due to the effects of the expansion wave[14] that is generated at the corner of the initiation tube and the driver section. Eventually, the deflagration wave transits to the detonation wave, resulting in the increase of the maximum pressure behind the detonation wave. This phenomenon is evident from the measured results of the propagation velocity of the detonation wave, which will be described later. The maximum pressure at measuring station DP8 is approximately 6.4 MPa, and this value is also equal to the pressure behind the C-J detonation wave, which is calculated assuming chemical equilibrium[15].

Figure 5 compares of the pressure histories measured at DP1 with the results of the KASIMIR shock tube simulation program[11]. The pressure histories obtained by the KASIMIR program show good agreement with experimental data, e.g., the value of the

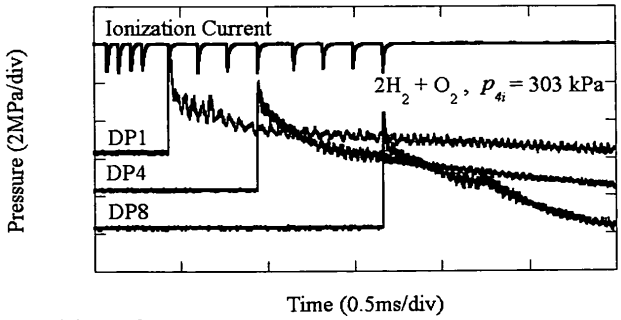

Fig. 4 Profiles of ionization current (upper) and pressure histories (lower), showing the propagation of detonation wave ($p_{4i}=303$ kPa, $\phi=1.0$)

maximum pressure behind the detonation wave, and the attenuation phenomena of the pressure by the Taylor expansion wave. The diaphragm is ruptured when the pressure becomes constant behind Taylor expansion wave, and this phenomenon is well simulated by the KASIMIR program.

Figure 6 shows the propagation velocity of the detonation wave obtained by measuring the time intervals in which the detonation wave propagates to two neighboring measuring stations. The horizontal axis is distance D from the ignition plug. This figure also shows the propagation velocities of the detonation wave when oxy-hydrogen gas is filled directly into the driver tube (▽) and when it is filled by using a mixing tank (○). The propagation velocity of the detonation wave is almost constant when the gas is filled by the mixing tank and is equal to the C-J detonation velocity of 2 850 m/s. However, when gas is filled directly into the driver tube and diffuses inside the tube, the propagation velocity of the detonation wave varies. This indicates that the mixing conditions for oxygen and hydrogen are critical factors that affect the propagation velocity of the detonation wave. The propagation velocity of the detonation wave decreases at D=1 000 mm because the combustion wave separates from the shock wave when the detonation wave transits from the initiation tube to the driver tube, as mentioned above. However, the detonation wave is reflected by the wall of the driver tube, and thus the propagation velocity of the detonation wave is increased to equal that of the C-J detonation velocity at D=1 500 mm.

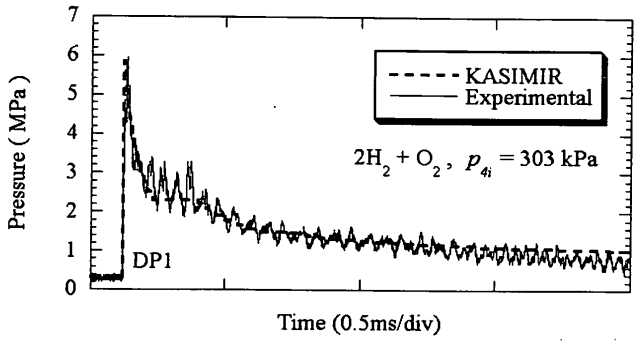

Fig. 5 Comparison of experimental and simulated pressure histories behind detonation wave (p_{4i}=303 kPa, ϕ=1.0)

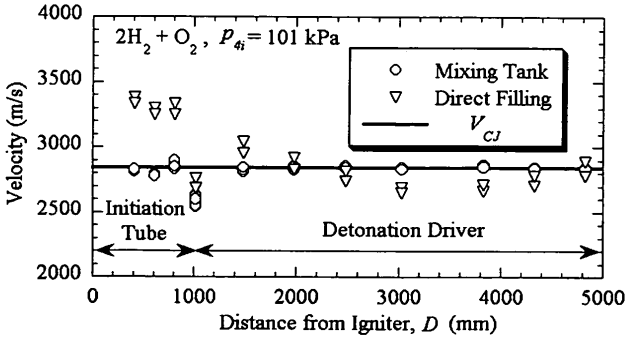

Fig. 6 Propagation velocity of detonation wave inside detonation driver. V_{CJ} indicates Chapman-Jouguet (C-J) detonation velocity (p_{4i}=101 kPa, ϕ=1.0)

3.3 Pressure histories in shock tube

Figure 7 exhibits pressure histories measured from SP1 through SP4 in a shock tube. The results were obtained under the conditions of initial pressure p_{4i}=303 kPa, p_1=11.3 kPa and equivalence ratio ϕ=1.0. Under these experimental conditions, the shock wave of propagation Mach number M_S=5.0 is obtained. It is observed that the pressure behind the shock wave decreases as the shock wave propagates. In the detonation-driven shock tube, high-pressure and high-temperature gases behind the detonation wave become reservoir gas for driving a shock wave; the length of the reservoir gas may not be sufficient and the expansion wave generated by the rupture of a diaphragm overtakes the shock wave. Therefore, the pressure histories measured at stations SP3 and SP4 are attenuated.

Figure 8 shows the relationship between Mach number of the shock wave M_S and the equivalence ratio ϕ, under the conditions of the initial pressure of driver gas p_{4i}=101 kPa and the initial pressure of driven gas p_1=11.3 kPa. The Mach number of the shock wave increases when the equivalence ratio is greater than unity. In the fuel-rich condition, ϕ>1.0, hydrogen remains after combustion, and the molecular weight of the driver gas decreases. The propagation Mach number of the shock wave has a maximum value at ϕ=1.7. This is because the temperature behind the detonation wave decreases and the temperature ratio as shown in Eq.(2) decreases.

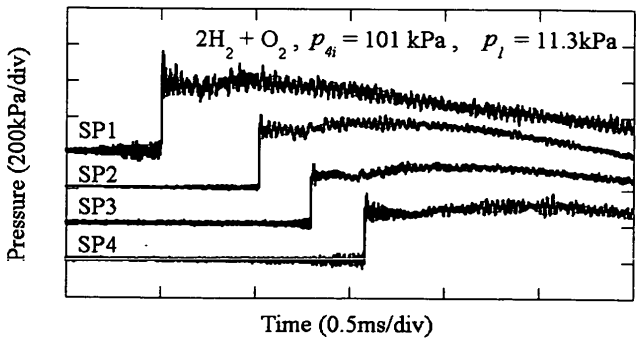

Fig. 7 Pressure histories of shock wave traveling inside shock tube (p_{4i}=303 kPa, p_1=11.3 kPa, ϕ=1.0)

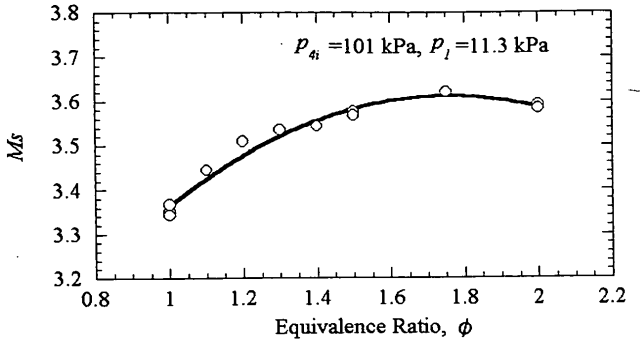

Fig. 8 Relationship between equivalence ratio, ϕ and Mach number of the shock wave M_S (p_{4i}=101 kPa, p_1=11.3 kPa)

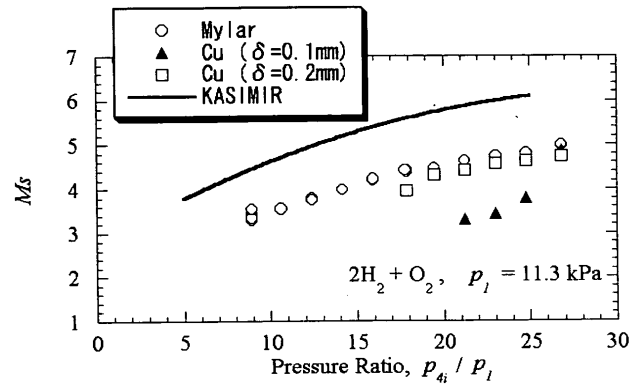

Fig. 9 Relationship between pressure ratio p_{4i}/p_1 and Mach number of the shock wave M_S (p_1=11.3 kPa, ϕ=1.0)

3.4 Variation of shock Mach number with difference in diaphragm material

The Mach number of the shock wave may vary by changing the material used for fabricating the diaphragm installed between the driver tube and the shock tube, since the rupture period of the diaphragm may vary. Figure 9 shows the relationship between Mach number of the shock wave M_S and non-dimensional pressure ratio of the driver gas to the driven gas, p_{4i}/p_1. This figure also shows the results obtained using Mylar film and copper disk plate, as well as those obtained by varying the depths of the ditch, δ= 0.1 mm (▲) and δ=0.2 mm (□), on the surface of the copper disk plate. In this figure, the solid line shows the results of the KASIMIR shock tube simulation program[11]. The propagation Mach number of the shock wave M_S monotonically increases as the pressure ratio p_{4i}/p_1 increases when Mylar film is used as the diaphragm material. The depth of the ditch on the copper plate is important when copper plate was used as the diaphragm material. The Mach number of the shock wave is smaller when a copper plate of δ=0.1 mm is used than when Mylar film is used.

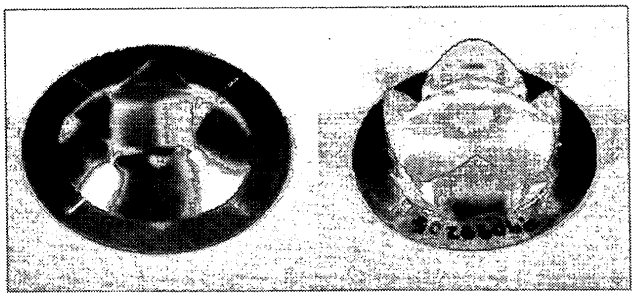

(a) (b)

Fig. 10 Copper disk after rupture (70 mm diameter and 0.4 mm thickness) depth of ditch (a) δ=0.1 mm, and (b) δ=0.2 mm (p_{4i}=240 kPa, p_1=11.3 kPa, ϕ=1.0)

The Mach number of the shock wave estimated by the KASIMIR shock tube simulation program is markedly different from the experimental results. This may be explained as follows: (i) The KASIMIR shock tube simulation program assumes that the diaphragm opens instantaneously and does not take into account the rupture period of the diaphragm; (ii) The KASIMIR program does not calculate the effects produced by the separation of the detonation wave from the combustion wave and the shock wave at the conjugation section between the initiation tube and the driver tube.

Figure 10(a) shows a photograph of the ruptured copper plate with δ=0.1 mm. The small depth of the cross-ditch on the copper plate is not sufficient for opening and the ruptured area is small (opening area: 20.3%). Since the opening area is small, the release period of the driver gas becomes long and the shock wave of relatively high Mach number is not generated. On the other hand, Fig. 10(b) shows the ruptured copper disk plate with δ=0.2 mm. The rupture of the copper disk plate is fine (opening area 100%), and the Mach number of the shock wave is a relatively high value. Therefore, it is confirmed that the Mach number of the shock wave is markedly changed by the rupture conditions of the diaphragm, and is relevant to the pressure ratio between the driver tube and the shock tube.

4. Summary

A detonation-driven shock tube was designed and setup in a laboratory. Preliminary experiments were undertaken in order to clarify the performance of the detonation-driven shock tube by measuring the pressure and ionization current behind the detonation wave. The results are summarized as follows.

(1) The propagation velocity of the detonation wave was equivalent to the theoretical value of the

Chapman-Jouguet detonation velocity, when oxy-hydrogen gas was filled into the detonation-driver tube via mixing tank.

(2) The propagation Mach number of the shock wave was maximum when the equivalence ratio of oxy-hydrogen was approximately 1.7.

(3) A copper disk plate was used as diaphragm material, and experiments were carried out by varying the depth of the cross-ditch on the surface of the copper plate. The Mach number of the shock wave was varied, and it was found to be related to the rupture conditions of the copper disk, which were changed by the depth of the cross-ditch and the pressure ratio between driver gas and driven gas p_{4i}/p_1.

(4) The propagation Mach number of the shock wave was estimated by the KASIMIR shock tube simulation program and the results were compared with the experimental values. It was found that the KASIMIR program gave higher estimates than the experiments.

Acknowledgements

The authors would like to thank to Messrs. T. Yoshihashi and T. Yamazaki for their technical assistance in the experiments.

References

(1) Archer, R.D. and Saarlas, M., An Introduction to Aerospace Propulsion, (1996), pp. 1-35, Prentice-Hall, Inc.

(2) Anderson, J.D. Jr., Hypersonic and High Temperature Gas Dynamics, (1989), pp. 1-28, McGraw-Hill, Inc.

(3) Kubota, N. and Kuwahara, T., Ramjet Technology, (in Japanese), (1996), pp. 1-25, The Nikkan Kogyo Shimbun, Ltd.

(4) Takafuji, R., Yamanaka, A., Obara, T., Cai, P. and Ohyagi, S., A Study on Behavior of Diffracted Shock Wave (1st Report, Process of Shock Wave Diffraction and Reflection), Trans. Jpn. Soc. Mech. Eng.,(in Japanese), Vol. 65, No. 639, B (1999), pp. 3602-3607.

(5) Ikui, T. and Matsuo, K., Mechanics of Shock Waves, (in Japanese), (1983), pp. 149-199, Corona Pub.

(6) Yu, H.R., Esser, B., Lenartz, M., Grönig, H., Gaseous Detonation Driver for a Shock Tunnel, Shock Waves, Vol. 2 (1992), pp. 245-254.

(7) Yu, H.R., Zhao, W., Li, Z.F., Gu, J.H. and Zhang, X.Y., Preliminary Experimental Results of the Detonation-Driven Shock Tube, Proc. 20th Int. Symp. Shock Waves, Vol. II (1995), pp. 1509-1514.

(8) Lenartz, M., Wang, B. and Grönig, H., Development of a Detonation Driver for a Shock Tunnel, Proc. 20th Int. Symp. Shock Waves, Vol. I (1995), pp. 153-158.

(9) Jiang, Z., Yu, H.R. and Takayama, K., Investigation into Converging Gaseous Detonation Drivers, Proc. Symp. Shock Wave, Jpn 1999, (1999), pp. 639-642.

(10) Nettleton, M.A., Gaseous Detonations: Their Nature, Effects and Control (1987), pp. 42-68, Chapman and Hall Ltd.

(11) Stoßwellenlabor, RWTH Aachen, KASIMIR Shock Tube Simulation Program, Instruction Manual, (1993).

(12) Ohyagi, S., Yajima, S., Obara, T. and Yoshihashi, T., Transition Processes from Deflagration to Detonation Waves (Effects of Obstacles), Trans. Jpn. Soc. Mech. Eng.,(in Japanese), Vol. 59, No. 567, B(1993), pp. 3552-3556.

(13) Watanabe, S., Obara, T., Yoshihashi, T. and Ohyagi, S., Visualization of Initiation Processes of Film Detonation, Trans. Jpn. Soc. Mech. Eng.,(in Japanese), Vol. 63, No. 612, B(1997), pp. 2700-2706.

(14) Hoshi, S., Tsutsumi, S., Yoshihashi, T., Obara, T. and Ohyagi, S., A Study on Diffraction of Detonation Waves, Proc. Symp. on Shock Wave, Jpn 1999, (in Japanese), (1999), pp. 313-316.

(15) Hikita, T. and Akita, K., Outline of Combustion, Physics and Chemistry of Flames, (in Japanese), (1971), pp. 126-131, Corona Pub.